Combined Use of Stereospecific Deuteration, NMR, Distance Geometry, and Energy Minimization for the Conformational Analysis of the Highly δ Opioid Receptor Selective Peptide [D-Pen^2,D-Pen^5]enkephalin

Henry I. Mosberg,* Katarzyna Sobczyk-Kojiro, Pullachipatti Subramanian, Gordon M. Crippen, Kondareddiar Ramalingam, and Ronald W. Woodard

Contribution from the College of Pharmacy, University of Michigan, Ann Arbor, Michigan 48109. *Received May 26, 1989*

Abstract: Comparison of ^{1}H and ^{13}C NMR parameters for the cyclic, conformationally restricted, δ opioid receptor selective enkephalin analogue Tyr-D-Pen-Gly-Phe-D-Pen ([D-Pen^2,D-Pen^5]enkephalin, DPDPE) in aqueous versus dimethyl sulfoxide (DMSO) solution indicates that this peptide adopts similar conformations in these solvents. This suggestion that the conformation of DPDPE is relatively environment independent allows conclusions regarding the receptor-bound conformation of this peptide to be drawn from studies performed on experimentally convenient DMSO solutions of the peptide, alone. Accordingly, 2D NOESY experiments were conducted on DPDPE in DMSO, and the observed interproton interactions were utilized for the quantitative calculation of the appropriate interproton distances. A commonly encountered limitation, the general inability to stereospecifically assign diastereotopic and enantiotopic hydrogens within the amino acid residues, which results in increased error limits for calculated distances involving such hydrogens, was overcome by the synthesis of stereospecifically deuterated amino acids (2*S*,3*R*)-[3-^{2}H]tyrosine, (2*S*,3*S*)-[4,4,4-^{2}H$_3$]penicillamine, (*R*)-[2-^{2}H]glycine, and (2*S*,3*R*)-[3-^{2}H]phenylalanine and their incorporation into DPDPE. As a result *all* resonances in the ^{1}H NMR spectrum of DPDPE were assignable, and more stringent interproton distances were calculated from the observed NOE interactions. These interproton distances were employed as distance constraints for distance geometry calculations of conformations consistent with the experimental data. Energy minimization of conformers generated by distance geometry calculations was performed by using the AMBER force field, and the resulting low-energy conformers were reexamined for agreement with distance constraints and other conformation-dependent NMR parameters. From these studies a conformer was identified that displayed significantly lower energy than all others found while maintaining good agreement with experimental data. Details of this model conformer and comparisons with recently proposed conformations for DPDPE are discussed.

Many native peptide hormones and neurotransmitters are relatively small, flexible molecules that, due largely to this flexibility, can interact with several distinct receptor types, each requiring different ligand conformations, to initiate different physiological events. In order to unravel the physiological roles played by these heterogeneous receptors, it is necessary to develop analogues of the native peptides that display enhanced receptor selectivity. Such selective ligands with more narrow spectra of pharmacological actions might then be of potential clinical relevance. One approach toward development of more receptor-selective ligands is the incorporation of conformational restrictions that may allow the resulting analogues to interact favorably with one type of receptor but not others. Conformationally restricted analogues afford the additional advantage of being more amenable to conformational analysis because they are less subject than are more flexible peptides to conformational averaging and because their solution conformations are more realistically extrapolated to the active, binding conformation. Further, a conformationally restricted and receptor-selective analogue allows insight into the particular structural and conformational features necessary for interaction with a specific receptor type.

One example of such a conformationally restricted, receptor-selective peptide is the enkephalin analogue [D-Pen^2,D-Pen^5]-enkephalin (DPDPE), Tyr-D-Pen-Gly-Phe-D-Pen, where Pen, penicillamine, is β,β-dimethylcysteine. DPDPE, which is conformationally restricted due to cyclization via the side-chain sulfurs of the penicillamine residues and due to the *gem*-dimethyl substitutents on these residues, displays extremely high selectivity for the δ opioid receptor.[1] As a result, conformational analysis of DPDPE provides the opportunity for the elucidation of specific structural and conformational features necessary for activity at δ opioid receptors. Indeed, several studies have been reported in which conformational analysis of DPDPE has been the focus. We have reported previously[2] the results of preliminary ^{1}H NMR experiments that indicate a preferred conformation, in aqueous solution, stabilized by an intramolecular hydrogen bond in which the D-Pen^5 amide hydrogen participates. Recent reports have presented more detailed models of the active conformation of DPDPE. Using computational methods and comparison with putative active conformations of other δ receptor selective enkephalin analogues, Loew and co-workers proposed a specific compact conformation for DPDPE stabilized by intramolecular hydrogen bonding.[3] A quite different model was proposed by Hruby et al.,[4] based upon NMR data including qualitative interproton distance information from NOESY experiments, computer-assisted model building, and energy minimization. We present here an alternate model for the solution, and by extrapolation the active, conformation of DPDPE and compare this model with those previously proposed. In arriving at our model, we have employed NMR data including quantitative interproton distances determined from NOE buildup rates and have used these interproton distances as constraints for distance geometry calculations of conformations consistent with these constraints. Conformations resulting from distance geometry calculations were energy minimized to identify low-energy candidate conformers consistent with experimental data. A common shortcoming of NOE-derived distance constraints for small peptides such as DPDPE is the uncertainty imposed by the inability to stereospecifically assign resonances from diastereotopic or enantiotopic atoms. When one proton in a pair of diastereotopic or enantiotopic protons exhibits a specific NOE interaction, this lack of stereospecific assignment manifests itself as an imprecise internuclear distance. For DPDPE many such specific NOE interactions are observed. We have addressed

(1) Mosberg, H. I.; Hurst, R.; Hruby, V. J.; Gee, K.; Yamamura, H. I.; Galligan, J. J.; Burks, T. F. *Proc. Natl. Acad. Sci. U.S.A.* **1983**, *80*, 5871-5874.

(2) Mosberg, H. I. *Int. J. Pept. Protein Res.* **1987**, *29*, 282-288.

(3) Keys, C.; Payne, P.; Amsterdam, P.; Toll, L.; Loew, G. *Mol. Pharmacol.* **1988**, *33*, 528-536.

(4) Hruby, V. J.; Kao, L. F.; Pettitt, B. M.; Karplus, M. *J. Am. Chem. Soc.* **1988**, *110*, 3351-3359.

0002-7863/90/1512-822$02.50/0

and alleviated this problem by synthesizing stereospecifically deuterated D-Pen, Gly, L-Tyr, and L-Phe and incorporating them into DPDPE. We report here the resulting NMR assignment of *all* resonances of the ^{1}H NMR spectrum of DPDPE and the use of these assignments for the development of a model for the δ receptor binding conformation of DPDPE.

Experimental Section

Peptide Synthesis. DPDPE and stereospecifically deuterium-labeled DPDPE were prepared by using solid-phase peptide synthesis methodology as previously described for DPDPE.[1] Chloromethylated polystyrene resin cross-linked with 1% divinylbenzene was used as the solid support. *tert*-Butyloxycarbonyl (Boc) protection was employed for the α-amino functions of all amino acids, and *p*-methylbenzyl protection was used for the sulfur-containing side chains of Pen residues. Cleavage from the resin and simultaneous deprotection were effected by treatment with HF, and the resulting linear, free sulfhydryl containing peptides were cyclized by oxidation with $K_3Fe(CN)_6$ to yield the corresponding cyclic, disulfide-containing analogues. All peptides were purified by semipreparative HPLC on a Vydac 218TP C-18 column (2.2 cm × 25 cm) as previously described.[5] Purified peptides were >98% pure as determined by analytical HPLC monitored at four different wavelengths, and all peptides had appropriate molecular weights as assessed by fast atom bombardment mass spectrometry.

Synthesis of Stereospecifically Deuterated Amino Acids. The four stereospecifically deuterated amino acids used in this study were prepared as follows:

(*R*)-[2-^{2}H]Glycine was prepared, by the method previously described by one of our laboratories,[6] from commercially available [α-^{2}H]*p*-anisaldehyde by reduction with (*R*)-*B*-isopinocampheyl-9-borabicyclo-[3.3.1]nonane (*R*-Alpine-Borane), a reagent first described by Midland et al.[7] and available from Aldrich Chemical Co., to give the desired *S*-deuterated arylmethyl alcohol in 82% enantiomeric excess (ee) (uncorrected for percent deuteration or percent ee of the starting Alpine-Borane) as determined by the method described by Parker.[8] The alcohol was converted to the corresponding chiral arylmethylphthalimido derivative having the opposite configuration at the arylmethylene carbon atom (*R*) via the procedure of Mitsunobu et al.[9] The phthaloyl group was removed via sodium borohydride reduction of the succinimide ring followed by acid hydrolysis.[10] The amine was converted to the *t*-Boc derivative via standard methods,[11] and the resulting (1*R*)-[1-^{2}H]-*N*-(*tert*-butyloxycarbonyl)-*p*-methoxybenzylamine was subjected to ruthenium tetraoxide oxidation[12] and (2*R*)-[2-^{2}H]-*N*-(*tert*-butyloxycarbonyl)glycine obtained. The optical purity (80% ee) of the chiral glycine was verified by the method of Armarego et al.[13]

(2*S*,3*R*)-[3-^{2}H]Phenylalanine and (2*S*,3*R*)-[3-^{2}H]tyrosine were prepared by standard asymmetric hydrogenation methodology,[14] namely, the use of hydrogen gas to reduce the appropriately deuterium-labeled α-benzamidocinnamic acid derivative, utilizing the asymmetric reduction catalyst (cycloocta-1,5-diene)[(*R*,*R*)-1,2-ethanediylbis[(*o*-methoxyphenyl)phenylphosphine]]rhodium tetrafluoroborate (*R*,*R*-dipamp). The deuterated *Z* dehydro amino acid derivatives (*Z*)-2-benzamido-*p*-methoxy[3-^{2}H]cinnamic acid and (*Z*)-2-benzamido[3-^{2}H]cinnamic acid needed for these hydrogenations were obtained from the corresponding azlactones by mild acid hydrolysis.[15] The (*p*-methoxyphenyl)azlactone derivative was prepared via the condensation of *p*-methoxy[α-^{2}H]benzaldehyde (commercially available) with hippuric acid and the phenylazlactone derivative by condensation of [α-^{2}H]benzaldehyde (commercially available) with hippuric acid by classical Erlenmeyer–Plochl methods.[16] Both the deuterated (*Z*)-cinnamic acid derivatives were subjected to hydrogenation in methanol over *R*,*R*-dipamp to give the desired 2*S*,3*R* 3-^{2}H aromatic amino acid. The optical purity was estimated by two different methods, first via optical rotation, assuming that the deuterium substitution has only a minor effect on optical rotation and noting that since the hydrogenation is cis, the optical purity at the β-center should be the same as the optical purity at the α-center (in several studies directed at determining if there is any isomerization about the double bond during the metal-catalyzed hydrogenation, only the *E* isomer has shown any tendencies to rearrange[14,17]), and second via ^{1}H NMR since the β-hydrogen atoms are diastereotopic and thus display chemical shift nonequivalence (the *pro-S* proton of *N*-benzoylphenylalanine (or *N*-benzoyltyrosine) resonates at low field and the *pro-R* proton at high field[17,18]).

(2*S*,3*S*)-[4,4,4-^{2}H$_3$]Penicillamine was prepared from stereospecifically deuterated 6-(phenoxyacetamido)-(3*S*)-penicillinic acid *S*-sulfoxide benzyl ester. The two major critical steps are the stereospecific oxidation of the 6-(phenoxyacetamido)-(3*S*)-penicillinic acid benzyl ester to give exclusively the *S*-sulfoxide[19] (commercially available from Sigma Chemical Co.) and the specific exchange of only the *pro-S* methyl protons of the *S*-sulfoxide of 6-(phenoxyacetamido)-(3*S*)-penicillinic acid benzyl ester with D_2O via a sulfoxide–sulfenic acid equilibrium.[20] The trideuterated penicillin derivative was deprotected via catalytic hydrogenation to remove the benzyl ester and treated with PBr_3 to deoxygenate the sulfoxide. The trideuterated 6-(phenoxyacetamido)-(3*S*)-penicillinic acid thus formed was converted to the desired chiral deuterated penicillamine derivative via standard degradation methods with hydrazine.[21] The exact experimental procedure along with the details for the synthesis of the diastereomer (2*S*,3*R*)-[4,4,4-^{2}H$_3$]penicillamine will appear elsewhere.

NMR Studies. ^{1}H and ^{13}C NMR spectra were recorded on a General Electric GN500 spectrometer operating at 500 MHz for proton and 125.6 MHz for carbon. Peptide concentrations for 2D NMR experiments were ca. 18 mM in 0.5-mL solutions of D_2O or H_2O/D_2O (90:10) adjusted to pH 3.0 (uncorrected meter reading) with CD_3COOD or of 100.00% Me_2SO-d_6 without pH adjustment. Concentrations of deuterium-labeled DPDPE used for 1D NMR stereospecific assignments were 3–5 mM. Except for temperature dependence studies, all experiments were performed at 298 K. Chemical shifts are reported as parts per million (ppm) downfield of internal 2,2,3,3-tetradeuterio-3-(trimethylsilyl)propionic acid sodium salt (TSP-d_4).

Homonuclear chemical shift correlations were determined from double-quantum-filtered (DQF) COSY experiments[22] processed in absolute value mode. Spectral widths were 3000 Hz in each dimension. Data sets of 1K spectra compiled from 32 transients for each of 256 values of the incremented delay t_1 yielded, after zero filling, 512 × 512 real matrices. Prior to Fourier transformation the data were apodized in both dimensions by a nonshifted sine bell function.

Heteronuclear ^{1}H–^{13}C connectivities were examined through heteronuclear COSY experiments. Spectral widths of 15 800 Hz (^{13}C) and 4900 Hz (^{1}H) were employed to generate 1K × 128 data sets that were zero filled to yield final 2K × 1K data sets. Exponential multiplication was applied, prior to Fourier transformation, to the ^{13}C data to improve sensitivity.

Pure phase absorption mode NOESY spectra were obtained by the method of States et al.,[23] using the standard pulse sequence RD–90°–t_1–90°–τ_m–90°–acq with an additional homospoil pulse introduced during the mixing time, τ_m, to eliminate scalar couplings. A relaxation delay (RD) of 3 s was used, and 1K spectra were generated from 48 scans collected for each of 256 incremented values of t_1 which yielded, after zero filling, 512 × 512 matrices. Spectral widths of 3000 Hz were

(5) Mosberg, H. I.; Omnaas, J. R.; Goldstein, A. *Mol. Pharmacol.* **1987**, *31*, 599–602.
(6) Ramalingam, K.; Nanjappan, P.; Kalvin, D. M.; Woodard, R. W. *Tetrahedron* **1988**, *44*, 5597–5604.
(7) Midland, M. M.; McDowell, D. C.; Hatch, R. L.; Tramontano, A. J. *J. Am. Chem. Soc.* **1980**, *102*, 867–869.
(8) Parker, D. *J. Chem. Soc., Perkin Trans. 2* **1983**, 83–87.
(9) Mitsunobu, O.; Wada, M.; Sano, T. *J. Am. Chem. Soc.* **1972**, *94*, 679–680.
(10) Osby, J. O.; Martin, M. G.; Ganem, B. *Tetrahedron Lett.* **1984**, *25*, 2093–2096.
(11) Moroder, L.; Hallett, A.; Wunsch, E.; Keller, O.; Wersin, G. *Hoppe-Seyler's Z. Physiol. Chem.* **1976**, *357*, 1651–1653.
(12) Carlsen, P. H. J.; Katsuki, T.; Martin, V. S.; Sharpless, K. B. *J. Org. Chem.* **1981**, *46*, 3936–3938.
(13) Armarego, W. L. F.; Millory, B. A.; Pendergast, W. *J. Chem. Soc., Perkin Trans. 1* **1976**, 2229–2237.
(14) Koenig, K. E.; Knowles, W. S. *J. Am. Chem. Soc.* **1978**, *100*, 7561–7564.
(15) Vineyard, B. D.; Knowles, W. S.; Sabacky, M. J.; Bachman, G. L.; Weinkauff, D. J. *J. Am. Chem. Soc.* **1977**, *99*, 5946–5952.
(16) Adams, R., Ed. *Organic Reactions*; John Wiley & Sons Inc.: New York, 1946; Vol. 3, pp 198–239.
(17) Detellier, C.; Gelbard, G.; Kagan, H. B. *J. Am. Chem. Soc.* **1978**, *100*, 7556–7561.
(18) Trimble, L. A.; Reese, P. B.; Vederas, J. C. *J. Am. Chem. Soc.* **1985**, *107*, 2175–2177.
(19) Cooper, R. D. G.; Demarco, P. V.; Cheng, J. C.; Jones, N. D. *J. Am. Chem. Soc.* **1969**, *91*, 1408–1415. Cooper, R. D. G.; Hatfield, L. D.; Spry, D. O. *Acc. Chem. Res.* **1973**, *6*, 32–40 and references therein.
(20) Cooper, R. D. G. *J. Am. Chem. Soc.* **1970**, *92*, 5010–5011.
(21) Pliva Pharmaceutical and Chemical Works. British Patent 1,472,052, 1977.
(22) Piantini, U.; Sorensen, O. W.; Ernst, R. R. *J. Am. Chem. Soc.* **1982**, *104*, 6800–6801. Shaka, A. J.; Freeman, R. *J. Magn. Reson.* **1983**, *51*, 169–173. Rance, M.; Sorensen, O. W.; Bodenhausen, G.; Wagner, G.; Ernst, R. R.; Wuthrich, K. *Biochem. Biophys. Res. Commun.* **1983**, *117*, 458–479.
(23) States, D. J.; Haberkorn, R. A.; Ruben, D. J. *J. Magn. Reson.* **1982**, *48*, 286–292.

employed in each dimension, and a nonshifted sine bell function was applied in each dimension prior to Fourier transformation. Cross-peak and diagonal volumes were extracted from unsymmetrized data sets obtained from eight separate experiments in which τ_m varied from 50 to 500 ms.

Carbon longitudinal relaxation times, T_1, were determined by using the inversion recovery method RD–180°–τ–90°–acq. A relaxation delay of 6 s was used in each 16K spectrum of spectral width 13000 Hz. Spectra arising from 600 scans were obtained for each of 18 separate values of the variable delay τ. T_1 values were calculated by using a least-squares polynomial fit.

Distance Geometry Calculations. Two different distance geometry embedding algorithms were used to locate conformations consistent with the NMR-derived distance constraints. For the majority of the calculations, the basic EMBED algorithm,[24] similar to that employed in Havel's DISGEO[25] program, was used. The remaining calculations employed a second algorithm, linearized embedding,[26] a variation in which the molecule is described in terms of local coordinate systems attached to the various rigid moieties, and the metric matrix embedding takes place in terms of the axes of these coordinate systems, rather than in terms of the atom coordinates directly. In either case, the initial objective was to determine a sampling of conformations, if any, that were consistent with the experimental geometric constraints arising from NOE-derived interproton distances, as well as a priori fixed bond lengths, fixed bond angles, and van der Waals radii. Stereospecific assignments of the otherwise ambiguous β-methyl protons of the D-Pen residues and α protons of Gly improved considerably upon the customary use of pseudoatoms[27] by significantly reducing the upper bounds of interproton distances involving these protons. Stereospecific assignments of the β hydrogens of the Tyr and Phe residues were less informative, since no NOE interaction favoring just one of the pair of β protons of either residue was observed, so pseudoatoms midway between the β protons were employed and 0.82 Å was added to the upper bounds. For interactions involving aromatic protons of Tyr or Phe, a pseudoatom located at the center of the ring was employed and interproton distances were increased by 2.4 Å. For Pen residues, while the β-methyls were distinguished, the three hydrogens in a given methyl all contribute to a given NOE. Therefore a pseudoatom at the center of mass of the three hydrogens for each methyl was introduced, and any upper bounds on such distances were increased by 0.94 Å. For any distance experimentally determined by NOEs and not involving a pseudoatom, we conservatively interpreted the interatomic distance to be constrained by the experimental value ±0.5 Å.

In addition to the NMR-derived distance constraints, the usual standard bond length and bond angle distance equality constraints and otherwise lower bounds given by the sum of the van der Waals atomic radii were used, as were chirality constraints for each of the chiral and prochiral centers in the molecule. Aromatic rings and peptide amide groups were constrained to be planar by the introduction of degenerate chiral constraints, but the interatomic distance bounds across each peptide amide bond were given cis/trans extreme values, so that peptide bonds could be either cis or trans.

The linearized embedding program made use of exactly the same geometric constraints as did the ordinary EMBED algorithm, except that for technical reasons the peptide bonds were fixed to be planar and trans, instead of also allowing cis. The linearized embedding program was able to more easily detect experimental constraints that were redundant, given the rigid valence geometry and minor inconsistencies between the experimental and a priori constraints. As explained in the Results section, these inconsistencies were so minor that numerous conformations having no violation greater than 0.5 Å of any distance constraint and no chirality violation were easily produced. A structure having worse errors was noted as "unsuccessful" and discarded.

Energy Minimization. Conformers of DPDPE produced by distance geometry embedding satisfy all the geometric constraints but are not necessarily energetically optimal, although gross atomic overlaps have been avoided. Therefore, the conformational energies of these structures were subsequently refined by calculations using the AMBER version 3.0 united-atom force field.[28] Since penicillamine is not a standard amino acid, some additional atom–atom interaction parameters had to be supplied. These were easily extrapolated from similar parameters and from the crystal structure of penicillamine.[29] The experimental distance constraints were not included in the force field, and consequently, the energy-minimized structures tended to have slightly higher violations of the constraints.

Energy minimizations were performed on the isolated DPDPE molecule with no solvation and with a dielectric constraint of 1. Our reasoning is that, since this molecule is extremely compact due directly to its covalent structure, virtually all interactions are between pairs of atoms separated by other atoms of the same molecule without intervening solvent. Except for details of the side-chain conformations of Tyr and Phe, one would then expect the molecular conformational preferences to be little affected by solvation and the dielectric constant of the solvent, an expectation supported by the comparison of NMR parameters observed in aqueous vs DMSO solutions (see below). To test the validity of this approach, several distance geometry generated structures were energy minimized by use of a dielectric constant of 49 (that of DMSO). The resulting conformations differed only slightly from those arising from the use of a dielectric constant of 1.

Table I. ^{1}H NMR Chemical Shifts of DPDPE in Aqueous (a) and DMSO (b) Solutions

	soln	Tyr[1]	D-Pen[2]	Gly[3]	Phe[4]	D-Pen[5]
NH	a		8.20	8.52	8.47	7.40
	b		8.60	8.57	8.88	7.23
H_α	a	4.39	4.19	*pro-R* 3.54	4.52	4.43
				pro-S 4.35		
	b	4.25	4.54	*pro-R* 3.21	4.41	4.33
				pro-S 4.40		
H_β (*pro-R*)	a	3.15			3.03	
	b	2.96			2.82	
H_β (*pro-S*)	a	3.02			3.15	
	b	2.74			3.09	
H_γ (*pro-R*)	a		1.48			1.34
	b		1.37			1.33
H_γ (*pro-S*)	a		0.84			1.29
	b		1.00			1.29
H_{ar} (ortho)	a	6.87			7.26	
	b	6.68			7.25	
H_{ar} (meta)	a	7.16			7.36	
	b	7.10			7.26	
H_{ar} (para)	a				7.31	
	b				7.26	

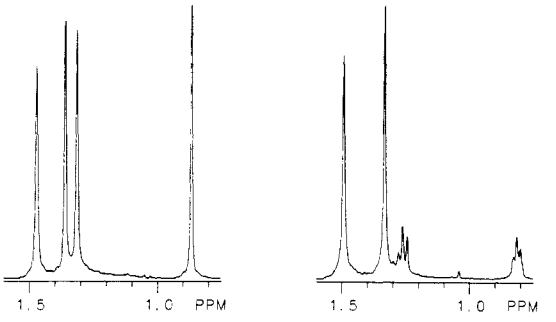

Figure 1. Penicillamine methyl proton region of the ^{1}H NMR spectra of DPDPE (left) and [d_3-D-Pen^2,d_3-D-Pen^5]enkephalin (right) in D_2O solution.

Results

We have previously reported the assignments, except for prochiral protons, of the ^{1}H NMR spectrum of DPDPE in aqueous solution at 270 MHz.[2,30] Table I shows the chemical shifts observed for DPDPE in aqueous solution at 500 MHz, which are in complete agreement with our previously reported values, as well as corresponding data for DPDPE in DMSO solution. In both solvents assignments were independently determined by a combination of DQF-COSY, sequential assignments from NOESY techniques, and homonuclear difference decoupling where necessary. Stereospecific assignments of the diastereotopic β protons of Tyr[1] and of Phe[4], the diastereotopic β-methyl protons of D-Pen[2] and of D-Pen[5], and the enantiotopic α protons of Gly[3] were de-

(24) Crippen, G. M.; Havel, T. F. *Distance Geometry and Molecular Conformation*; Research Studies Press: New York, 1988.
(25) Havel, T. F. *QCPE Bull.* **1986**, *6* No. 507.
(26) Crippen, G. M. *J. Comput. Chem.*, in press.
(27) Wuthrich, K.; Billeter, M.; Braun, W. *J. Mol. Biol.* **1983**, *169*, 949–961.
(28) Weiner, S. J.; Kollman, P. A.; Case, D. A.; Singh, U. C.; Ghio, C.; Alagona, G.; Profeta, S.; Weiner, P. *J. Am. Chem. Soc.* **1984**, *106*, 765–784.
(29) Rosenfeld, R. E., Jr.; Parthasarathy, R. *Acta Crystallogr. B* **1975**, *31*, 462–468.
(30) Mosberg, H. I.; Omnaas, J. R.; Ramalingam, K.; Woodard, R. W. *J. Labelled Compd. Radiopharm.* **1987**, *24*, 1265–1271.

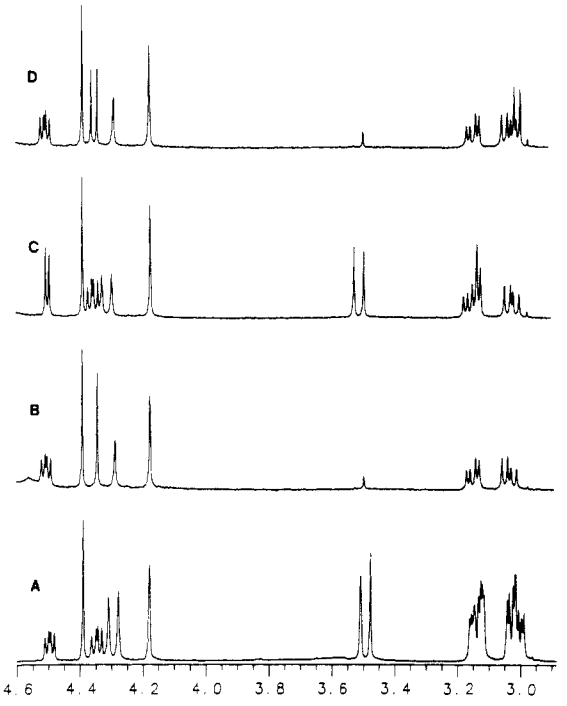

Figure 2. ^{1}H NMR spectra (α and β proton regions) of DPDPE (A), [[3,3-$^2H_2$]Tyr^1,2*R*-[^{2}H]Gly^3]DPDPE (B), [3*R*-[^{2}H]Phe^4]DPDPE (C), and [3*R*-[^{2}H]Tyr^1,2*R*-[^{2}H]Gly^3]DPDPE (D) in D_2O solution.

termined directly from the ^{1}H spectra of [3*S*-[4,4,4-[$^2H_3$]]-D-Pen^2,3*S*-[4,4,4-[$^2H_3$]]-D-Pen^5]DPDPE ([d_3-D-Pen^2,d_3-D-Pen^5]-DPDPE) (Figure 1) and of [3*R*-[^{2}H]Tyr^1,2*R*-[^{2}H]Gly^3]DPDPE and [3*R*-[^{2}H]Phe^4]DPDPE (Figure 2). As can be seen from Figure 1, the downfield methyl resonance of each Pen residue of [d_3-D-Pen^2,d_3-D-Pen^5]DPDPE is unchanged from that of unlabeled DPDPE, which allows the unequivocal assignment of these resonances as arising from the (3*R*)-methyl groups of the Pen residues. The observed complex and broadened multiplet structures of the residual (3*S*)-methyl resonances are due to contributions from the incompletely deuterated species $-CHD_2$ and $-CH_2D$. Figure 2 displays the α- and β-proton region of the ^{1}H spectra of DPDPE (Figure 2A), [3*R*-[^{2}H]Phe^4]DPDPE (Figure 2C), and [3*R*-[^{2}H]Tyr^1,2*R*-[^{2}H]Gly^3]DPDPE (Figure 2D). From inspection of Figure 2, parts A and D, it is clear that the downfield Gly α resonance must be due to the 2*S* proton. Elucidation of the assignments of the β region of Phe^4 and Tyr^1, which overlap, is aided by Figure 2B, which depicts this portion of the spectrum for [[3,3-$^2H_2$]Tyr^1,2*R*-[^{2}H]Gly^3]DPDPE in which only Phe^4 β resonances are observed. From Figure 2, parts B and D, it is clear that the Tyr 3*S* proton resonance of [3*R*-[^{2}H]Tyr^1,2*R*-[^{2}H]-Gly^3]DPDPE is at δ = 3.02 ppm (and thus the Tyr *pro-R* resonance in DPDPE is at δ = 3.15 ppm). Figure 2, parts B and C, likewise shows that the 3*S* resonance of Phe^4 in [3*R*-[^{2}H]-Phe^4)DPDPE is at δ = 3.15 ppm (and thus the Phe *pro-R* resonance in DPDPE is at δ = 3.03 ppm). It should be pointed out that Figures 1 and 2 depict spectra taken in D_2O solutions. Similar straightforward assignments follow from spectra obtained in DMSO solutions.

Assignments of the ^{13}C spectrum of DPDPE are presented in Table II. The majority of the assignments were determined by heteronuclear COSY experiments on unlabeled DPDPE; however, once again the stereospecifically deuterated analogues proved useful, allowing unequivocal assignment of all the penicillamine γ carbons in both aqueous and DMSO solutions and of the β carbons of Phe and Tyr in DMSO, in which these chemical shifts differ. Comparison of ^{13}C chemical shifts (Table II) and ^{1}H chemical shifts (Table I) of DPDPE in aqueous vs DMSO solutions reveals excellent agreement of these parameters between these solvents. Other than differences for amide proton chemical shifts, which reflect differing hydrogen-bonding capabilities of the two solvents, significant chemical shift differences are observed for

Table II. ^{13}C NMR Chemical Shifts of DPDPE in Aqueous (a) and DMSO (b) Solutions

	soln	Tyr^1	D-Pen^2	Gly^3	Phe^4	D-Pen^5
C_α	a	54.49	61.09	42.34	56.75	62.72
	b	53.40	58.51	41.61	56.10	61.70
C_β	a	36.30	50.66		36.30	52.36
	b	36.22	50.83		36.82	52.12
C_γ (*pro-R*)	a		27.21			26.23
	b		27.69			25.68
C_γ (*pro-S*)	a		26.02			26.95
	b		25.40			27.26
$C_{2,6}$	a	127.56			130.95	
	b	126.38			130.43	
$C_{3,5}$	a	116.30			129.28	
	b	115.23			128.86	
C_4	a	155.41			129.06	
	b	156.46			128.84	
C_1	a	125.74			136.30	
	b	125.00			137.96	

Table III. Vicinal Coupling Constants, $J_{NH\alpha CH}$, and Allowed Φ Angles for DPDPE in Aqueous (a) and DMSO (b) Solutions

residue	soln	$J_{NH\alpha CH}$, Hz	Φ, deg[a]
D-Pen^2	a	7.8	155; 85; −40; −80
	b	8.5	150; 80; −50; −75
Gly^3 (NHα_{pro-R})	a	4.3	110; 15; −60; −180
	b	5.0	100; 20; −70; −170
Gly^3 (NHα_{pro-S})	a	8.4	155; 85; −60 ± 30
	b	7.9	160; 80; −60 ± 30
Phe^4	a	6.0	90; 25; −75; −165
	b	7.0	80; 35; −85; −160
D-Pen^5	a	8.6	155; 90; −50; −70
	b	8.4	150; 85; −45; −75

[a] Calculated from ref 31.

Table IV. Vicinal Coupling Constants, $J_{\alpha\beta}$, and Calculated Rotamer Populations, P_i, for DPDPE in Aqueous (a) and DMSO (b) Solutions

	soln	Tyr^1	Phe^4
$J_{\alpha\beta(pro-S)}$, Hz	a	9.5	6.0
	b	9.2	4.5
$J_{\alpha\beta(pro-R)}$, Hz	a	6.5	9.0
	b	6.9	10.2
P_I (χ = −60°),[a] %	a	35	58
	b	39	69
P_{II} (χ = 180°),[a] %	a	62	31
	b	60	17
P_{III} (χ = 60°),[a] %	a	3	11
	b	1	14

[a] Calculated from ref 32.

the D-Pen^2 α carbon and hydrogen resonances and for the Tyr β and aromatic proton resonances. These differences probably reflect conformational differences of the extracyclic tyrosine residue in the two solvents. The chemical shift variation of the D-Pen^2 residue can be attributed to different ring current effects arising from the differing conformations of the tyrosine aromatic ring. These ring current effects have been shown to result in the observed high-field chemical shift of the *pro-S* methyl resonance and low-field chemical shift of the *pro-R* methyl resonance of the D-Pen^2 residue.[2] It is also observed that the Gly *pro-R* α-proton resonance is shifted further upfield in DMSO compared with aqueous solution. In both solvents this resonance owes its upfield position to diamagnetic shielding by neighboring carbonyl groups (see below), and thus the rather large chemical shift difference observed between solvents might reflect a rather small conformational difference, since this shielding effect is strongly dependent on the relative orientations of the shielded proton and shielding carbonyl. The data of Tables I and II suggest that, at the very least, the four amino acid cyclic portion of DPDPE assumes very similar conformations in aqueous and in DMSO solutions.

Additional evidence of similar conformations in the two solvents is presented in Tables III–V. As shown in Table III, similar values

Table V. Temperature Dependence of Amide Proton Chemical Shifts for DPDPE in Aqueous (a) and DMSO (b) Solutions

	soln	D-Pen[2]	Gly[3]	Phe[4]	D-Pen[5]
$-d\delta/dT$, ppb/K	a	6.6	5.2	5.1	0.8
	b	3.2	2.6	5.1	−0.3

of $J_{NH\alpha CH}$, the coupling constant between the amide proton and α proton of each residue, are observed in both solvents. The value of this coupling constant is a function of ϕ, the dihedral angle about the C^O–N^α–C^α–C^O bond,[31] and thus similar values between the two solvents are suggestive of similar conformations. Allowed values of ϕ ($\pm\sim 20°$) corresponding to each observed $J_{NH\alpha CH}$ are also shown in Table III. Note that stereospecific assignment of the Gly[3] α-proton resonances allows the unequivocal assignment of the coupling constants between the Gly NH and each prochiral α proton, which decreases the number of allowed ϕ angles to those consistent with both observed couplings. For the Gly residue of DPDPE in DMSO solution only ϕ values of ca. −70° and ca. 90° display such consistency. Table IV compares the values observed in DMSO and aqueous solutions for $J_{\alpha\beta}$, the coupling constant between the α and β protons, observed for Tyr[1] and for Phe[4]. By analogy with $J_{NH\alpha CH}$, this coupling constant depends upon the conformation about the C^α–C^β bond; however, since greater conformational freedom is expected for amino acid side chains within a peptide, values of $J_{\alpha\beta}$ are more commonly related to the populations of the three lowest energy, staggered rotamers about this bond.[32] The calculated rotamer populations are also presented in Table IV. Ordinarily, some ambiguity exists regarding the assignment of these populations to a particular rotamer since generally the β protons are not stereospecifically assigned. The stereospecific assignments of the Tyr and Phe β protons afforded by the synthesis of stereospecifically deuterated Tyr and Phe allow unequivocal determination of the coupling constants $J_{\alpha\beta}$ and $J_{\alpha\beta'}$ and consequently of the rotamer populations,[33] which are virtually identical in the two solvents. The assignment of the Phe β protons is in agreement with that expected for internal aromatic residues in a polar solvent,[34] while that of the β protons of the amine-terminal Tyr would not be predicted a priori.

The observed temperature dependencies of amide proton chemical shifts, an indicator of the accessibility of these protons to solvent, are shown in Table V. In both aqueous and DMSO solutions insensitivity of amide proton chemical shifts to changes in temperature reflects inaccessibility to the hydrogen-bonding solvent[35] and is usually interpreted, for small peptides, as arising from an intramolecular hydrogen bond, although a non-hydrogen-bonding amide located in a solvent-impenetrable region is also possible. From Table V it is evident that in both aqueous and DMSO solutions only the D-Pen[5] amide proton is solvent inaccessible. Once again this agreement of conformation-dependent NMR parameters between the two solvents suggests highly similar conformations of DPDPE in aqueous and DMSO solutions.

The finding that DPDPE assumes similar conformations in aqueous and DMSO solutions is significant for two reasons. First, such similarity lends credence to the extrapolation of conformational features of the peptide in solution to the active, receptor-bound conformation since it is evidence for a preferred, environment-independent conformation. Second, it allows NOESY experiments of DPDPE to be performed without loss of relevance in DMSO, which, compared with aqueous solvent, provides more intense cross peaks (due to a more favorable rotational correlation time) and facile observation of all interactions in a single experiment without complications arising from a strong H_2O solvent resonance. Figure 3 shows a sample NOESY contour plot for DPDPE in DMSO solution. While qualitative interproton distance information can be deduced from a single NOESY experiment in the absence of spin diffusion effects, quantitative distances and corroboration of the absence of spin diffusion effects require the determination of NOE buildup rates from a series of NOESY experiments in which the mixing time, τ_m, is varied.[36] Furthermore, accurate distance determination requires that the individual proton relaxation times, T_1, be known for the molecule or, alternatively, that molecular reorientation can be described by a single correlation time.[37,38] The validity of the latter assumption can best be assessed by examining the ^{13}C T_1 values for DPDPE, since for proton-bearing carbons this relaxation is dominated by dipolar interactions with these protons, and the observation of similar values of NT_1, where N is the number of directly bonded hydrogens, for individual carbons indicates that molecular motions can be described by a single correlation time. Carbon-13 T_1 values for DPDPE are shown in Table VI. When the number of directly bonded hydrogens is taken into account, the resulting NT_1 values for the backbone α carbons are in the range 290–440 ms (NT_{1av} = 371 ± 41 ms). Values of NT_1 for the $C_{2,6}$ and $C_{3,5}$ aromatic carbons of Tyr and Phe and for the C_4 aromatic carbon of Phe are similar (NT_{1av} = 410 ± 54 ms), and NT_1 values for the side-chain β carbons of Phe and Tyr lie just beyond this range (NT_{1av} = 512 ± 52 ms). NT_1 values of the Pen methyl carbons, which are influenced by rotation about the C^β–C^γ bond, are somewhat larger. Interestingly, relaxation

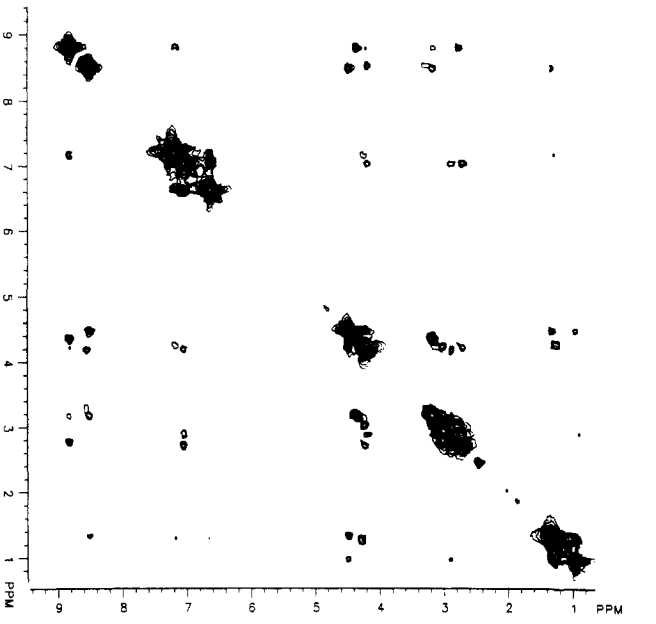

Figure 3. Sample NOESY contour for DPDPE in DMSO solution. A symmetrized data set is shown.

Table VI. ^{13}C Relaxation Times, T_1 (ms), of DPDPE in DMSO Solution

	Tyr[1]	D-Pen[2]	Gly[3]	Phe[4]	D-Pen[5]
C_α	381	290	221	392	350
C_β	230	1280		282	2110
C_γ (*pro-R*)		151			289
C_γ (*pro-S*)		331			209
$C_{2,6}$	340			499	
$C_{3,5}$	405			352	
C_4	2390			456	
C_1	973			1460	

(31) Bystrov, V. F. *Prog. Nucl. Magn. Reson. Spectrosc.* **1976**, *10* (Part 2), 41–81.
(32) Pachler, K. G. R. *Spectrochim. Acta* **1964**, *20*, 581–587.
(33) Stereospecific assignment of the Tyr and Phe β hydrogens could also be obtained from C^O–H^β cross-peak intensities of H, C COLOC experiments (Kessler, H.; Griesinger, C.; Wagner, K. *J. Am. Chem. Soc.* **1987**, *109*, 6927–6933). Such experiments generally require large quantities of peptide.
(34) Kobayashi, J.; Higashijima, T.; Miyazawa, T. *Int. J. Pept. Protein Res.* **1984**, *24*, 40–47.
(35) Deslauriers, R.; Smith, I. C. P. In *Biological Magnetic Resonance*; Berliner, L. J., Reuben, J., Eds.; Plenum Press: New York, 1980; Vol. 2, pp 243–344.
(36) Wagner, G.; Wuthrich, K. *J. Magn. Reson.* **1979**, *33*, 675–680. Bothner-By, A. A.; Noggle, J. A. *J. Am. Chem. Soc.* **1979**, *101*, 5152–5155.
(37) Noggle, J. H.; Schirmer, R. E. *The Nuclear Overhauser Effect, Chemical Applications*; Academic Press: New York, 1971. Bruch, M. D.; Noggle, J. H.; Gierasch, L. M. *J. Am. Chem. Soc.* **1985**, *107*, 1400–1407.
(38) Keepers, J. W.; James, T. L. *J. Magn. Reson.* **1984**, *57*, 404–426.

Table VII. Interproton Distances for DPDPE Calculated from NOESY Experiments

from		to		
residue	proton	residue	proton	*r*, Å
Tyr	αH	D-Pen²	NH	2.76
Tyr	βH	D-Pen²	Me (*pro-S*)	3.15
Tyr	βH	Tyr	Ar (meta)	2.64
D-Pen²	NH	D-Pen²	Me (*pro-S*)	3.61
D-Pen²	αH	D-Pen²	Me (*pro-R*)	2.52
D-Pen²	αH	D-Pen²	Me (*pro-S*)	2.76
D-Pen²	αH	Gly	NH	2.28
D-Pen²	αH	Gly	αH (*pro-R*)	3.46
D-Pen²	Me (*pro-R*)	Gly	NH	2.66
Gly	NH	Gly	αH (*pro-R*)	2.83
Gly	αH (*pro-R*)	Gly	αH (*pro-S*)	1.75 (ref)
Gly	αH (*pro-R*)	Phe	NH	3.40
Gly	αH (*pro-S*)	Phe	NH	2.28
Phe	NH	Phe	βH	2.76
Phe	NH	D-Pen⁵	NH	2.71
Phe	αH	D-Pen⁵	NH	2.43
Phe	βH	D-Pen⁵	Me (*pro-S*)	2.92
D-Pen⁵	NH	D-Pen⁵	Me (*pro-R*)	2.54
D-Pen⁵	αH	D-Pen⁵	Me (*pro-R*)	2.96

of the D-Pen² *pro-R* methyl carbon is considerably more efficient than the other Pen methyls. These findings are consistent with the interpretation that, to a reasonable approximation, the motional behavior of DPDPE can be described by a single correlation time, τ_c. While this may not be strictly correct for the Pen methyls, it has been shown that, in general, failure to take into account internal rotation of methyl groups leads to only minor errors in NOE-derived distances.[38]

Eight NOESY spectra were recorded with mixing times of 50–500 ms to obtain bulidup rates of the NOE cross peaks by using unsymmetrized 2D NOE data sets. Initial buildup rates for short mixing times (≤80 ms) were used to calculate interproton distances, r_{ij}, by comparison with the initial buildup rate between the Gly α and α′ protons with the known interproton distance, r_{kl}, of 1.75 Å by using the relationship[37]

$$r_{ij} = r_{kl}[\sigma_{kl}/\sigma_{ij}]^{1/6}$$

where σ_{kl}/σ_{ij}, the ratio of the cross-relaxation parameter between the reference Gly α and α′ protons to that between spins *i* and *j*, is determined from the cross-peak buildup rates. The ^{1}H resonances of these Gly protons display a large chemical shift nonequivalence and thus exhibit cross peaks well separated from the diagonal. Table VII summarizes the interproton distances calculated in this fashion for DPDPE in DMSO solution. As can be seen from Table VII, 20 interproton interactions, 13 of which specifically involve prochiral α protons of Gly or prochiral methyls of Pen, are observed and give rise to a set of 20 interproton distances used as constraints for distance geometry calculations.

As described above, the experimentally determined interproton distances plus or minus the estimated error limit of 0.5 Å were used as upper and lower distance bounds, respectively, for distances between uniquely determined protons, while larger bounds were necessary for pseudoatoms. From these and covalent constraints, EMBED produced 63 successful random structures at a success rate of only ca. 7%, which demonstrates how severely the experimental, rigid valence geometry, and van der Waals constraints interact to restrict the range of allowed conformations. Linearized embedding yielded 4 successes in 20 tries using the same constraints. Neither program ever produced a conformer that agreed perfectly with all constraints. This may be due to slight errors in the experimentally determined distances or may reflect the existence of some conformational averaging in solution, such that the experimental observations do not arise from a single conformer. Distance geometry generated structures were considered unsuccessful if any distance constraint violation exceeded 0.5 Å. While few of the 67 successful conformers were degenerate, many were quite similar and could be grouped into distinct families. Energy minimization (see below) of members within a structural family gave rise to correspondingly similar structures of similar energy.

Table VIII. Low-Energy Conformations of DPDPE

		model					
residue		I	II	III	III′	Hruby	Loew
Tyr¹	φ						
	ψ	−36	150	155	163	164	172
	ω	178	−176	−173	−177	−173	−173
	χ^1	−62	−179	69	−173	−163	−163
	χ^2	96	−125	−69	−115	51	58
Pen²	φ	−79	135	142	149	111	137
	ψ	−129	−29	−153	−153	14	−152
	ω	171	180	−173	−175	173	−173
	χ^1	−88	−69	−82	−78	−180	−68
	χ^2	−175	−168	176	178	143	66
Gly³	φ	82	−80	96	78	−98	84
	ψ	−66	49	−130	−111	−18	−146
	ω	−171	176	−168	−164	177	175
Phe⁴	φ	−105	−153	−79	−85	−72	−82
	ψ	−53	−81	27	38	−46	84
	ω	−174	178	−178	172	−175	−163
	χ^1	−60	−54	63	−64	179	−179
	χ^2	−73	−86	93	105	68	63
Pen⁵	φ	140	131	76	61	83	65
	ψ						
	ω						
	χ^1	−85	−69	−91	−87	−70	−53
	χ^2	62	72	61	60	119	59
∠C–S–S–C		109	110	102	110	−110	173
energy, kcal/mol		−43.7	−43.8	−44.3	−51.5		

Energy minimization of structures generated from distance geometry calculations was performed, as discussed above, by using the AMBER force field. The resulting structures displayed, in general, more and greater distance constraint violations than did the distance geometry structures themselves. These violations primarily involved side-chain hydrogens, which suggests that motional averaging of these side chains may be significant.

Low-energy conformers (within 10 kcal/mol of the lowest energy structure) from AMBER calculations were examined for further agreement with NMR parameters by comparing AMBER-determined values for ϕ_i with those, shown in Table III, inferred from the measured values for $J_{NH\alpha CH}$. Only the three lowest energy conformers among these exhibit complete agreement (±20°, the estimated error in values determined from $J_{NH\alpha CH}$) with these values. Calculated values of φ, ψ, ω, and χ for these conformers are presented in Table VIII. Also shown for comparison in Table VIII are values for models proposed by Hruby et al.[4] and by Loew and co-workers.[3] In order to compare these models, at least in a qualitative fashion, with our own, the conformers proposed by these workers were constructed by using the molecular modeling program MIDAS[39] and subjected to the AMBER force field in the same manner as was used for the distance geometry structures. The resulting conformers were of comparable energy with the low-energy conformations I–III of Table VIII. It must be noted, however, that the conformers resulting from AMBER energy minimization of the structures reported by Hruby et al. and by Loew and co-workers, while similar to those reported by these groups, displayed significant differences. Nonetheless, the results suggest that the conformers reported here and those proposed by Hruby et al. and by Loew and co-workers are similarly energetically favorable. When subjected to the distance constraints inferred from the NOE results reported here, the conformer arising from AMBER energy minimization of the structure reported by Loew displayed similar agreement as models I–III, while the conformer arising from the Hruby model resulted in more and greater violations.

Discussion

Although stereospecific deuteration and consequent stereospecific assignment of all ^{1}H resonances of DPDPE increase the

(39) Ferrin, T. E.; Huang, C. C.; Jarvis, L. E.; Langridge, R. *J. Mol. Graphics* **1988**, *6*, 2–12. Ferrin, T. E.; Huang, C. C.; Jarvis, L. E.; Langridge, R. *J. Mol. Graphics* **1988**, *6*, 13–37.

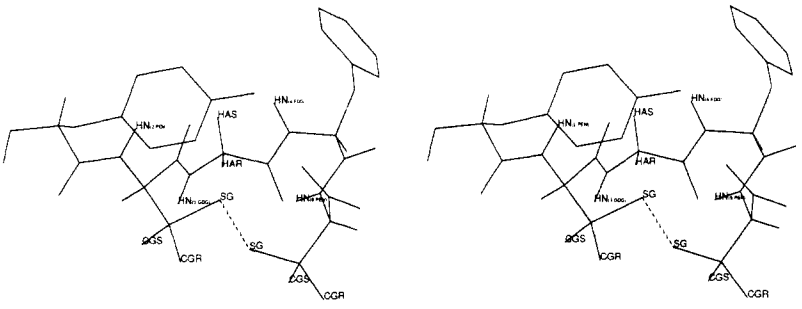

Figure 4. Stereoview of DPDPE conformer III′. Atoms labeled are sulfurs (SG) and *pro-S* (CGS) and *pro-R* (CGR) γ carbons of D-Pen^2 and D-Pen^5 residues, *pro-S* (HAS) and *pro-R* (HAR) α hydrogens of Gly^3, and all amide hydrogens (HN). The disulfide bond is denoted by a dashed line.

restrictiveness of the specific distance bounds determined from NOE interactions, it is clear from Table VIII that several quite different conformers are allowed. As noted above, energy minimizations were performed with the distance constraints removed, and consequently models I–III each exhibit two to three violations of individual constraints which exceed the distance geometry cutoff of 0.5 Å. Interestingly, each of these violations, which range from 1.1 to 1.7 Å, involves a β-methyl group on either penicillamine residue. Hruby et al.[4] observed low-energy conformers for DPDPE that displayed opposite chirality for the C^β–S–S–C^β dihedral angle while maintaining equivalent conformations elsewhere in the structure. Indeed, several distance geometry conformations were found in our study that similarly differed chiefly in an opposite chirality about the disulfide, although none of these were among the lowest energy group after energy minimization. These results suggest that flipping about the disulfide might occur in DPDPE in solution, leading to NOE-derived distances involving penicillamine methyl protons that represent average values for these distances. This change in disulfide chirality has been observed in molecular dynamics trajectories of DPDPE.[4]

In addition to agreement with interproton distance constraints, models I–III are all consistent with allowed values of ϕ determined from the coupling constants, $J_{NH\alpha CH}$, as shown in Table III. Additional examination of the consistency of these models with the NMR data allows some distinctions to be drawn among models I–III. As discussed above, the temperature dependence of amide proton chemical shifts of DPDPE in either aqueous or DMSO solution indicates that the D-Pen^5 amide proton is involved in an intramolecular hydrogen bond or is otherwise inaccessible to solvent. All other amide protons in DPDPE appear to be exposed to solvent. Models I–III are all consistent with the observed temperature insensitivity of the Pen^5 amide proton chemical shift. In all three models this amide proton is directed toward the center of the molecule, effectively buried in a solvent-inaccessible environment. In model III the Pen^5 amide is additionally involved in a hydrogen bond with the Gly^3 carbonyl, resulting in a C_7 turn centered around the Phe^4 residue. In models II and III all other amide protons are solvent accessible; however, in model I the Phe^4 amide participates in a hydrogen bond with the D-Pen^2 carbonyl. This hydrogen bond is inconsistent with the large temperature dependence observed for the Phe amide proton chemical shift, and as a result, model I must be considered a less attractive model for the solution conformation of DPDPE than are models II and III.

The large chemical shift nonequivalences observed for the enantiotopic α protons of the Gly^3 residue and the diastereotopic methyl protons of D-Pen^2 in DPDPE are clearly due to conformational effects, and any viable model must be able to account for these differences. From the use of stereospecifically deuterated residues it is clear that, in DMSO solution, the *pro-R* glycine α proton is that observed at 3.21 ppm while the *pro-S* α proton is found at 4.40 ppm. Originally we had proposed that the glycine chemical shift nonequivalence was a result of a ring current effect arising from the Phe^4 aromatic function;[2] however, subsequent studies by Hruby and co-workers[4] suggest that this nonequivalence is due to diamagnetic effects of carbonyl groups in DPDPE. Models II and III are consistent with this latter explanation since in model II the Gly *pro-R* α proton lies in a shielding region and the *pro-S* proton lies in a deshielding region of the Gly^3 carbonyl, while in model III the *pro-R* proton lies in a shielding and the *pro-S* proton in a deshielding region of the D-Pen^2 carbonyl group.

The chemical shift nonequivalence of the D-Pen^2 β-methyl protons has been proposed to arise from a ring current effect due to the Tyr^1 aromatic ring.[2] Both models II and III are consistent with this interpretation and with the stereospecific assignments resulting from the incorporation of stereospecifically deuterated penicillamine. In both of these models the *pro-S* D-Pen^2 methyl group is located within the shielding region of the Tyr aromatic ring, consistent with the observed upfield shift of this resonance.

As seen from Table VIII, model III predicts χ^1 angles for the Tyr^1 and Phe^4 side chains to be in the presumably energetically unfavorable gauche$^+$ ($\chi^1 = 60°$) orientation. Indeed, from the observed $J_{\alpha\beta}$ coupling constants, rotamer populations presented in Table IV indicate that this orientation is sparsely populated in both of these residues. Accordingly, model III was adjusted such that the Tyr χ^1 angle was 180° and the Phe χ^1 angle was −60°, consistent with the predominant rotamers evident in solution, and the resulting structure (which contains no additional distance constraint violations) was again subjected to energy minimization. This final optimized conformation, listed as model III′ in Table VIII and shown in Figure 4, is 7.2 kcal/mol lower in energy than model III, with which it is quite similar, maintaining all those features of model III discussed above, and is equally as consistent as models II and III with all NMR data. We thus propose model III′ as a working model for the solution and, by extrapolation, the δ receptor active conformation of DPDPE.

As is apparent from Table VIII, models I–III′ differ significantly from those proposed by Hruby and by Loew and their co-workers. In particular, the differences between our preferred model III′ and that of Hruby et al.[4] are considerable even though both studies used interproton distances determined from NOESY experiments in arriving at these models. In part this can be attributed to the improvements afforded the present study by the assignment of diastereotopic and enantiotopic protons and the resulting improvements in distance constraints defining the conformation. Additionally, differences in observed NOE interactions are also found. For example, Hruby et al.[4] observed NOESY cross peaks between the D-Pen^2 methyl protons and the aromatic ring protons of both Tyr^1 and Phe^4, while we observe only the former of these. Accordingly, the model proposed by Hruby et al. features these aromatic rings in close proximity, a feature absent in model III′. It should be noted, however, that such a close proximity between these aromatic rings is not itself precluded by our data and in fact model II in Table VIII, while still dissimilar from that proposed by Hruby et al., does contain such an arrangement. The proposed proximity of Phe^4, Tyr^1, and D-Pen^2 and D-Pen^5 side chains lends an amphiphilic character to the model of Hruby et al. that is not seen in our model. It is interesting to note that in model III′ the *pro-R* methyl of D-Pen^2 is directed away from the disulfide-containing ring structure in an exposed environment. We have previously proposed, on the basis of conformation–activity correlations with the conformationally similar analogues [D-Cys^2,D-Pen^5]enkephalin and [3*S*-Me-D-Cys^2,D-Pen^5]enkephalin, that the high δ receptor selectivity of DPDPE is due, at least in part, to an adverse steric interaction at the μ receptor binding site caused by the D-Pen^2 *pro-R* methyl group.[40] As a result DPDPE

displays high δ selectivity due to its poor μ receptor affinity. The location observed for this methyl group in model III' is consistent with this proposal.

Conclusions

The use of stereospecific deuteration to yield the *complete* assignment of the ^{1}H NMR spectrum, combined with quantitative interproton distance evaluation from NOESY cross-peak buildup rates and further coupled with distance geometry and energy minimization calculations, provides the best available experimental approach toward the elucidation of the solution conformation of DPDPE. These methods led in the present studies to the identification of one conformer consistent with the NMR data and of significantly lower energy than other allowed conformers. Nonetheless, it is likely that, even for a conformationally restricted peptide such as DPDPE, several similar and perhaps dissimilar conformations are significantly populated and that a weighted average is represented by the NMR spectrum. Such averaging must certainly be present in the more flexible side chains and may account for the observed small discrepancies in intramolecular distances involving side-chain protons between energy-minimized structures and NMR-derived constraints. Since it is quite clear that multiple low-energy conformers can be found that are consistent with experimental observations and display significant differences among themselves, it appears that further efforts to ascertain the solution conformation of DPDPE and, by extrapolation, its active conformation at the δ opioid receptor might best be directed toward uncovering common conformational features that are shared by similar conformationally restricted δ receptor selective peptides but are not found in other structurally related analogues with differing opioid activity. Such comprehensive studies utilizing an approach similar to that described here are in progress in our laboratories.

Acknowledgment. These studies were supported by USPHS Grants DA03910 (H.I.M.), GM37123 (G.M.C.), and GM36184 (R.W.W.) and by Grant DMB-8705006 (G.M.C.) from the National Science Foundation. The General Electric GN500 NMR spectrometer is supported by Grant RR-02415 from the USPHS and by funds from the University of Michigan College of Pharmacy.

Registry No. DPDPE, 88373-73-3; [α-^{2}H]-*p*-anisaldehyde, 19486-71-6; (*S*)-[α-^{2}H]-4-methoxybenzyl alcohol, 124176-47-2; (*R*)-*N*-[deuterio(4-methoxyphenyl)methyl]phthalimide, 124176-48-3; (*R*)-[α-^{2}H]-4-methoxybenzylamine, 124176-49-4; (*R*)-[α-^{2}H]-*N*-(*tert*-butoxycarbonyl)-4-methoxybenzylamine, 124176-50-7; (2*R*)-[2-^{2}H]-*N*-(*tert*-butoxycarbonyl)glycine, 124176-51-8; (2*S*,3*R*)-[3-^{2}H]-phenylalanine, 31262-73-4; (2*S*,3*R*)-[3-^{2}H]-tyrosine, 124176-52-9; (*Z*)-2-benzamido-*p*-methoxy-[3-^{2}H]-cinnamic acid, 39508-47-9; (*Z*)-2-benzamido-[3-^{2}H]-cinnamic acid, 39508-42-4; (*Z*)-2-benzamido-*p*-methoxy-[3-^{2}H]-cinnamic acid azlactone derivative, 39508-46-8; (*Z*)-2-benzamido-[3-^{2}H]-cinnamic acid azlactone derivative, 31348-62-6; hippuric acid, 495-69-2; [α-^{2}H]-benzaldehyde, 3592-47-0; trideuterated 6-(phenoxyacetamido)-(3*S*)-penicillinic acid (*S*)-sulfoxide benzyl ester, 124176-53-0; (2*S*,3*S*)-[4,4,4-^{2}H$_3$]penicillamine, 124176-54-1; trideuterated 6-(phenoxyacetamido)-(3*S*)-penicillinic acid, 124176-55-2; [d$_3$-D-Pen^2,d$_3$-D-Pen^5]enkephalin, 124176-44-9; [[3,3-^{2}H$_2$]Tyr^1,2*R*-[^{2}H]Gly^3]-DPDPE, 124176-45-0; [3*R*-[^{2}H]Phe^4]-DPDPE, 124199-94-6; (3*R*-[^{2}H]-Tyr^1,2*R*-[^{2}H]Gly^3)-DPDPE, 124176-46-1.

(40) Mosberg, H. I.; Haaseth, R. C.; Ramalingam, K.; Mansour, A.; Akil, H.; Woodard, R. W. *Int. J. Pept. Protein Res.* **1988**, *32*, 1-8.

In a Model C:G Base Pair, One Amino Group Rotates and the Other Does Not

Loren Dean Williams,† Nidhi Gupta Williams,‡,§ and Barbara Ramsay Shaw*,‡

Contribution from the Paul M. Gross Chemical Laboratory, Duke University, Durham, North Carolina 27706, and the Department of Biology, Massachusetts Institute of Technology, Cambridge, Massachusetts 02139. *Received May 31, 1989*

Abstract: Cytosine (C) and guanine (G) form Watson–Crick-type complexes in low-dielectric solvents. Dynamics of complexes between 3',5'-bis(triisopropylsilyl) derivatives of 2'-deoxynucleosides in deuteriochloroform were studied with 300-MHz ^{1}H NMR. We have determined rates of rotation about each amino bond of the C:G base pair. From the temperature dependence of the rates of amino group rotation, rotational activation enthalpies and entropies were calculated with line-shape and time-resolved techniques. For the amino group of G, the rotational activation enthalpy is equal to +10.6 ± 0.3 kcal/mol, and the rotational activation entropy ($\Delta S^{\ddagger}_{rotG}$) is equal to −2.5 ± 1.4 cal/(mol·T). As $\Delta S^{\ddagger}_{rotG}$ is nearly zero, the degree of disorder in the transition state is similar to that of the ground (base paired) state. We propose that rotation of the amino group of G proceeds within the base-paired state. In contrast, for the amino group of C, the rotational activation enthalpy is equal to +18.6 ± 1.3 kcal/mol, and the rotational activation entropy ($\Delta S^{\ddagger}_{rotC}$) is equal to +11.2 ± 3.5 cal/(mol·T). As $\Delta S^{\ddagger}_{rotC}$ is large, the degree of disorder in the transition state is greater than that of the ground state. We propose that rotation of the amino group of C proceeds through a transition state in which the base pair is disrupted. The results suggest that the two amino groups of the C:G base pair rotate via two different mechanisms. The amino group of G rotates within the base-paired state while the amino group of C rotates only during transient base-pair opening.

Although the ground state of DNA is close to the B conformation, DNA is a dynamic molecule which fluctuates between a variety of conformations. Amino groups in DNA rotate, and base pairs flip open and closed. DNA fluctuations are functionally significant, being factors in DNA recognition and reactivity. This paper describes one type of DNA fluctuation: rotation of the two amino groups of the cytosine–guanine base pair (Figure 1A). We have used ^{1}H NMR to study the mechanisms of amino proton exchange in a monomeric model system of DNA.

The properties of nucleic acid monomers have provided considerable insight into those of polymeric nucleic acids. The hydrogen-bonding interactions in the low-dielectric environment of the interior of polymeric nucleic acids[1,2] can be modeled by nucleic

* Address correspondence to this author.
† Massachusetts Institute of Technology.
‡ Duke University.
§ Current address: Department of Biological Chemistry and Molecular Pharmacology, Harvard Medical School, Boston, MA 02115.

(1) Levitt, M. *Cold Spring Harbor Symp. Quant. Biol.* **1982**, *47*, 251.

0002-7863/90/1512-829$02.50/0